Stability of cobalt supported on ZrO_2 catalysts for methane combustion

V.G. Milt, E.A. Lombardo*, M.A. Ulla

*Instituto de Investigaciones en Catálisis y Petroquímica, INCAPE (FIQ, UNL-CONICET), Santiago del Estero 2829,
3000 Santa Fe, Argentina*

Abstract

Cobalt supported catalysts were prepared by two different techniques: atomic layer epitaxy (ALE) and wet impregnation. Either ZrO_2 or La/ZrO_2 (La-doped ZrO_2) were used as supports. The solids were characterized by XRD, TPR and XPS before and after hydrothermal and catalytic stability tests (TOS: 150 h, 970 K). The most active catalysts were those in which cobalt was incorporated using the epitaxial growth technique. Moreover, the initial activity of cobalt supported on ZrO_2 by ALE was significantly higher than that on La/ZrO_2. But, after maintaining the former catalysts for 150 h at 970 K on stream (stability test), their initial high activities significantly decreased. On the other hand, when Co was supported on La-doped ZrO_2 the resulting catalysts became much more stable. Combining the catalytic results with the characterization information a simple model is proposed that rationalizes the behavior of these solids. © 2002 Elsevier Science B.V. All rights reserved.

Keywords: ALE; Cobalt; Zirconia; Methane combustion; Aging; Stability

1. Introduction

The catalytic combustion of natural gas, applicable to gas turbines, allows the reduction of NO_x emissions [1–3]. Catalysts used for this purpose must maintain a high activity over long periods. Nevertheless, there are limitations concerning materials that reduce the lifespan of high-temperature combustion catalysts. Both structural and catalytic durability are at stake. There are many publications concerning structural stability, where the catalysts are exposed to thermal treatments at very high temperatures [4–6].

Catalytic durability implies several special properties. The solids must be able to resist deactivation by sintering, loss by vaporization, deactivation by corrosion and erosion and delaminating [7]. Euzen et al. [8] studied the deactivation of palladium catalysts (Pd supported on stabilized aluminas). They analyzed the influence of methane/air ratio, palladium concentration and addition of promoters (ZrO_2, La_2O_3, CeO_2 and SiO_2) on the catalysts' activity (in terms of methane conversion), over periods of up to 60 h. CeO_2 seemed to improve the catalyst durability (either by increasing the PdO resistance to sintering and/or decreasing the PdO transformation into Pd) in laboratory aging tests. However, in pilot plant tests, the deactivation of the catalyst occurred very rapidly, indicating that the durability of Pd-based catalysts is strongly related to the operation conditions, and in particular, to catalyst temperature.

The rational to study supported cobalt catalysts is to find out an alternative to supported noble metal

* Corresponding author. Tel.: +54-342-4536861;
fax: +54-342-4536861.
E-mail address: nfisico@fiqus.unl.edu.ar (E.A. Lombardo).

catalysts for high-temperature operation, as is the case of hybrid burners [9–11]. Klavana et al. [12] performed long-term runs using supported substituted perovskites for the combustion of odorized natural gas. They found that the activity of $La_{0.66}Sr_{0.34}Ni_{0.29}Co_{0.69}Fe_{0.02}O_3$ (12%)/silica-alumina had not significantly changed for 10 days at 825 K, even though the feedstream contained 0.3 ppm methyl mercaptan (CH_3SH).

The study of catalytic activities for methane combustion at 1170 K over a series of $La_{1-x}Sr_xFeO_3$ ($0 \leq x \leq 0.5$) were reported by Batiot-Dupeyrat et al. [13]. The best performance was obtained with $La_{0.8}Sr_{0.2}FeO_3$. They also performed a stability test in which the conversion for all the samples decreased continuously with time on stream (22 h), mainly due to an important sintering. As the elements of this perovskite were supported on $BaAl_{12}O_{19}$ oxide a milder deactivation was observed. However, methane conversion was lower than that reached with unsupported perovskite accompanied by significant amounts of carbon monoxide.

In previous works [10,11] we found that cobalt supported on ZrO_2 and La-doped ZrO_2 by an epitaxial growth technique (atomic layer epitaxy) were good catalysts for the catalytic combustion of methane. Nevertheless, significant differences in the initial reaction rates were recorded when the cobalt was either supported on ZrO_2 or on La-doped ZrO_2. But, is this difference maintained after long-term experiments?

The goal of this work was to study the catalytic stability of several cobalt containing catalysts. They were obtained either by ALE or conventional impregnation techniques. Either plain ZrO_2 or La-doped zirconia were used as supports. The solids were maintained on stream at 970 K for more than 150 h. XRD, TPR, XPS and surface area measurements were the tools used in order to characterize the solids before and after the aging treatment.

2. Experimental

2.1. Catalyst preparation

ZrO_2 (previously calcined at 970 K in air) and La/ZrO_2 were used as supports. La-doped ZrO_2 was prepared by wet impregnation of ZrO_2 with a solution of lanthanum acetylacetonate ($La(acac)_3$) in anhydrous THF, evaporating the resulting suspension in an oven at 380 K for 12 h, followed by calcination in air at 770 K for 4 h. The final content of lanthanum was 9.6 wt.% La.

An epitaxial technique was used to incorporate cobalt onto these supports: atomic layer epitaxy (ALE). For the application of this method, a flow-type reactor operated at low pressure ($P \approx 1330 \, N \, m^{-2}$) was designed and built. More details about the ALE technique and apparatus are given elsewhere [11]. Over the corresponding treated support (at 770 K) cobalt acetylacetonate ($Co(acac)_3$) was sublimed and chemisorbed at 440 K for 1 h using N_2 as carrier, following a purge with N_2 at the same temperature. Then, calcination at 770 K for 1 h in air yielded the oxide species on the surface of the support. By repeating this cycle several times, the amount of cobalt anchored to the surface was increased.

For comparison, a solid containing 1.9 wt.% of Co on ZrO_2 was prepared by wet impregnation, dissolving $Co(acac)_2$ in isobutyl alcohol. After impregnation the solid was dried at 380 K for 12 h followed by calcination in air at 770 K for 4 h. All the catalysts were treated in air at 970 K for 4 h prior to being characterized and/or tested for methane combustion. Table 1 lists the catalysts used in the aging tests.

2.2. Characterization

X-ray diffractograms were obtained using an XD-D1 Shimadzu instrument with monochromator using Cu $K\alpha$ radiation at a scan rate of 1 per min. The BET surface area was determined in a Quantachrome Nova 1000 sorptometer.

TPR experiments were performed using an Okhura TS-2002 instrument equipped with a thermal conductivity cell (TCD). The catalysts (0.050 g) were pre-treated in oxygen at 620 K for 2 h. In order to eliminate bulk carbonates present in lanthanum-containing samples before running TPR experiments, catalysts were pre-treated with H_2 (5 vol.%)/Ar at 920 K for 30 min and then reoxidized with oxygen at 820 K for another 30 min. The experiments were done using 5% of hydrogen in argon, 40 cm^3 (STP) min^{-1}, with a heating rate of 10 K min^{-1}, from 320 to 1170 K. Under these conditions, the detection limit is 1 μmol H_2, equivalent to 0.1 μmol H_2/μmol Co, for a sample containing 1 wt.% Co.

Table 1
Catalysts

Catalyst[a]	Wt.% Co (x)	Preparation method	Number of ALE cycles	XRD phases[b]	S (m^2 g^{-1})
Co(x)La/ZrO$_2$	1.8	ALE	5	ZrO$_2$[c] and La$_2$O$_3$ (traces)	30 ± 3
	0.83	ALE	3		
	0.38	ALE	1		
Co(x)ZrO$_2$	1.9	ALE	5	ZrO$_2$[c]	30 ± 3
	0.95	ALE	3		
	0.42	ALE	1		
Co(x)/ZrO$_2$	1.9	Wet impregnation	–	ZrO$_2$[c]	30 ± 3

[a] Values between parentheses (x) indicate the Co wt.% determined by atomic absorption. The slash preceding the support indicates the use of the impregnation method, and no bar indicates the use of the ALE technique.

[b] Supports calcined at 970 K. Surface areas are not affected by the incorporation of cobalt.

[c] Monoclinic and tetragonal phases.

The XPS spectra were obtained at room temperature with a Shimadzu ESCA 750 instrument, using Al Kα radiation. XPS intensity ratios were calculated using the integrated areas (obtained with the software of the instrument) of the Co 2p$_{3/2}$ and La 3d$_{5/2}$ photoelectron lines (including the satellite peaks), and the sum of the overlapped integrated areas of Zr 3d$_{5/2}$ and Zr 3d$_{3/2}$ signals. The integrated areas were corrected taking into account the Scofield photoelectron cross-sections. The number of accumulated scans was 12 for both Co 2p and La 3d signals and it was 5 in the case of O 1s, C 1s and Zr 3d. These numbers of scans were enough to obtain a good signal-to-noise ratio. Each scan takes between 4 and 8 min. All the binding energies were corrected considering as reference the value of 530.0 eV for the O 1s signal (lattice oxygen).

2.3. Catalytic measurements

The solids were tested in a packed-bed tubular quartz reactor (i.d. 8 mm) with a 2 mm o.d. thermowell. The 0.010–0.050 g of catalyst were placed on a fritted quartz disk and covered by quartz wool. Mass flow controllers were used to meter the gas flows. The gas mixture consisted of 3 vol.% methane, 7.2 vol.% oxygen and nitrogen balance. The total volumetric gas flow was varied between 50 and 800 cm^3(STP) min^{-1}. The products were analyzed with an on-line gas chromatograph using a Porapak Q column and a thermal conductivity detector.

The methane combustion only yields carbon dioxide under our experimental conditions. Methane

conversion was thus calculated as the ratio between carbon dioxide concentration and the sum of methane and carbon dioxide concentrations (carbon compounds) at the reactor outlet. The reaction rates were calculated operating the reactor in a differential mode (always using methane conversion below 10%) as:

$$r = \frac{X_{CH_4} F_{CH_4}}{mS} (\mu mol\ s^{-1}\ m^{-2})$$

where X_{CH_4} is the methane conversion, F_{CH_4} the CH$_4$ flow rate [cm^3(STP) min^{-1}], m the catalyst mass (g), and S is the surface area of the catalyst (m^2[BET] g^{-1}) [10].

At 970 K there was no detectable methane conversion when flowing the reactant mixture through the quartz wool packed reactor (the detection limit of our system is 0.2% CH$_4$ conversion). Thus, the contribution of the homogeneous reaction is negligible.

The aging treatment consisted in keeping the catalysts on stream for a total time of 150 h at 970 K, using a total gas flow of 100 cm^3(STP) min^{-1}. At the beginning of each run, the temperature was set at 770 K and maintained at this temperature for 0.5 h. From the conversion data the initial reaction rate was calculated. After this, the temperature was raised to 970 K, and was maintained at this value for 12 h. Before the conversion measurements at 770 K, the reactor was cooled to room temperature in order to avoid any possible overheating of the catalytic bed and then the temperature was increased back to 770 K and was maintained at this temperature for 0.5 h. Then the methane conversion was measured and the rate was calculated. After

this, the temperature was raised again to 970 K and the reactor was maintained at this temperature for 24 h, and so on. This sequence was repeated up to 150 h on stream at 970 K.

3. Results

3.1. Catalytic activity and stability

Kinetic data obtained at 770 K were rigorously analyzed in order to detect the existence of both short and long range effect gradients in the reacting system. The detection of possible short-range gradients was analyzed according to the criteria proposed by Carberry [14] and Heck and Farrauto [3]. It was concluded that neither inter-phase concentration or temperature nor intra-phase concentration or temperature gradients were present under the tests conditions of our experiments. To calculate the reaction rates, CH_4 conversion values between 1 and 8% were used so as to minimize long-range effects. Complementary experiments indicated the absence of long-range effects. More details of the calculations made were reported elsewhere [11].

Fig. 1 shows the initial reaction rates obtained at 770 K for all the fresh catalysts. They can be divided into two groups: those supported on ZrO_2

Table 2
Short-term stability tests

Catalyst	Initial rate[a], $r \times 10^2$ ($\mu mol\, s^{-1}\, m^{-2}$)	Rate (10 h on stream)[b], $r \times 10^2$ ($\mu mol\, s^{-1}\, m^{-2}$)
Co(0.90)La/ZrO$_2$	29	27
Co(0.95)ZrO$_2$	47	30
Co(1.9)ZrO$_2$	64	51

[a] Initial reaction rate for CH_4 combustion at 770 K. Reactant composition: 3% CH_4, 7.2% O_2 and nitrogen balance.
[b] Reaction rate at 770 K after keeping the catalyst on stream at 770 K for 10 h.

and those supported on La-doped ZrO_2 (La/ZrO$_2$). Co(1.9)/ZrO$_2$, the solid prepared by wet impregnation, is included for comparison. From this figure, it is concluded that when the ALE method is used, cobalt supported on ZrO_2 is more active than cobalt supported on La-doped ZrO_2. The Co(1.9)ZrO$_2$ catalyst appears as the best formulation.

As a first attempt to investigate the stability of Co(x)ZrO$_2$ compared with the La-doped formulation, we carried out short-term tests at 770 K. Table 2 shows that Co(0.90)La/ZrO$_2$ is practically unaffected by this treatment while Co(x)ZrO$_2$ shows a significant deactivation. To ascertain if this trend is sustained in longer runs under more severe conditions, the solids were kept running for more than 150 h at 970 K. Fig. 2
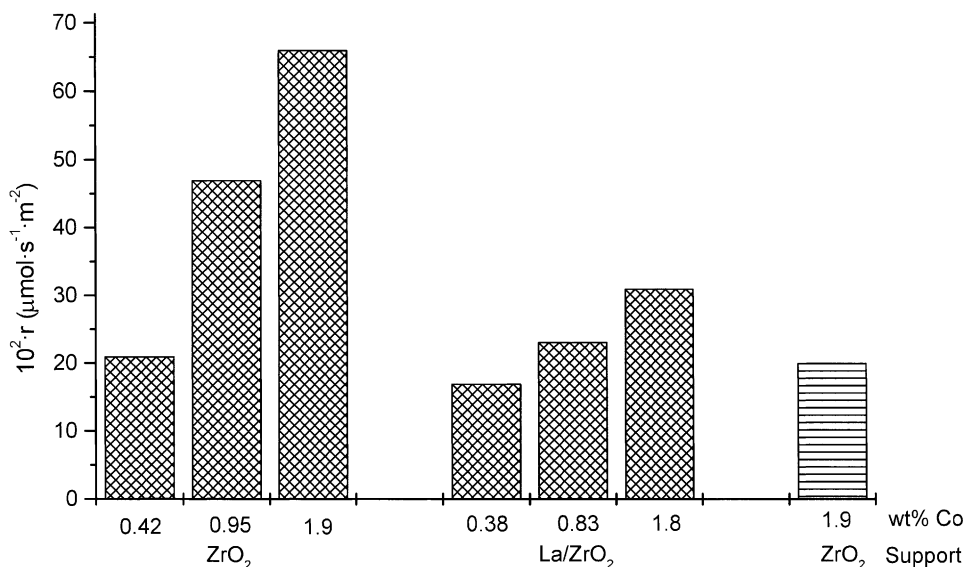

Fig. 1. Initial reaction rates for methane combustion at 770 K. Reactant composition: CH_4 3%, O_2 7.2%, balance N_2.
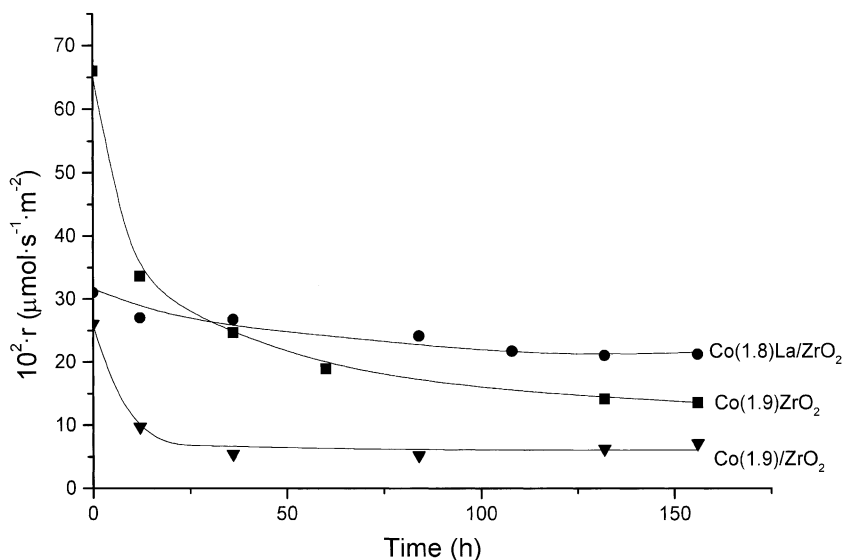
Fig. 2. Catalytic stability of solids prepared by different methods on ZrO_2 and La/ZrO_2. Test run at 970 K, rates measured at 770 K (see Section 2).

shows reaction rate profiles versus time on stream for the catalysts with the higher cobalt loadings, e.g. $Co(1.9)ZrO_2$, $Co(1.8)La/ZrO_2$ and $Co(1.9)/ZrO_2$. Note the quick deactivation that occurs when cobalt is supported on ZrO_2 by the epitaxial growth technique. In a similar way, the analogous solid prepared by wet impregnation also suffers a quick deactivation. In both cases, the rates decay to values lower than 50% of their initial levels after the catalysts underwent the aging treatment for only 12 h. The deactivation goes on at longer times and at the end of the treatment, the rates have reached 20–30% of their initial values. On the other hand, in the case of cobalt supported on La-doped ZrO_2, at the end of the severe treatment, the rate is still 67% of its initial rate value.

Fig. 3 shows how the solids with the highest and the lowest cobalt loadings supported on ZrO_2 ($Co(1.9)ZrO_2$ and $Co(0.42)ZrO_2$) behave along the aging treatment. Note that the activity drop of the latter is less pronounced than that of the former. A different behavior is observed for cobalt supported on La/ZrO_2. The shape of the aging curves of $Co(1.8)La/ZrO_2$ and $Co(0.83)La/ZrO_2$ are almost identical (Fig. 4). This could indicate that in this case the active sites formed would be the same for both solids, being more abundant in the catalyst with higher cobalt loading.

3.2. Crystalline phases and BET surface area

The XRD pattern of ZrO_2 indicates the presence of both the monoclinic and the tetragonal phases, while for La-doped ZrO_2 (La/ZrO_2) traces of La_2O_3 were also detected. There is no formation of $La_2Zr_2O_7$ within the limits of detection of this technique.

Table 1 summarizes the XRD results for all supported cobalt catalysts, $Co(x)ZrO_2$, $Co(x)/ZrO_2$ and $Co(x)La/ZrO_2$ after calcination at 970 K. The absence of XRD reflection lines corresponding to cobalt containing phases suggests that cobalt species do not have long-range order in these systems.

The surface area of the supports (ZrO_2 and La/ZrO_2) was $30 \, m^2 \, g^{-1}$. After cobalt addition (by ALE or wet impregnation techniques), no significant surface area changes were observed for all the catalysts (Table 1). The surface area of the catalysts after 150 h on stream (aged catalysts) could not be measured due to the small amount of catalyst used in our kinetic experiments. So in order to study the surface area stability of the solids, $Co(0.42)ZrO_2$ and $Co(0.38)La/ZrO_2$ were treated at 970 K for more than 150 h in a flow of steam saturated air (3% H_2O). After this treatment the BET surface areas did not change.
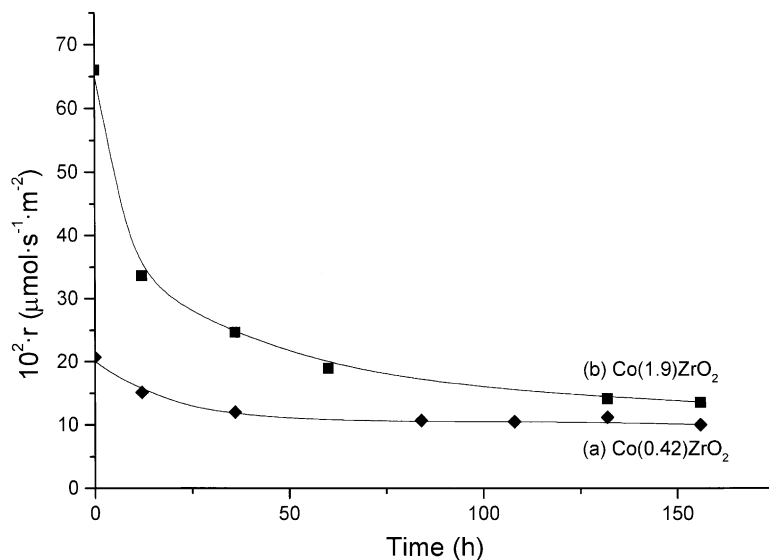
Fig. 3. Increasing the number of ALE cycles affects the stability of cobalt supported on plain zirconia. (a) One ALE cycle, (b) five ALE cycles.

3.3. Reducibility

Fig. 5 shows the hydrogen consumption in the TPR experiments for the fresh $Co(1.8)La/ZrO_2$ and $Co(1.9)ZrO_2$ catalysts. Similar TPR profiles were obtained for the other fresh samples. These catalysts contain cobalt species reducible at temperatures below 800 K. The peak at 420–470 K could be associated with O_2 chemisorbed on Co^{2+} centers [11]. Besides, there are cobalt species that are not reduced
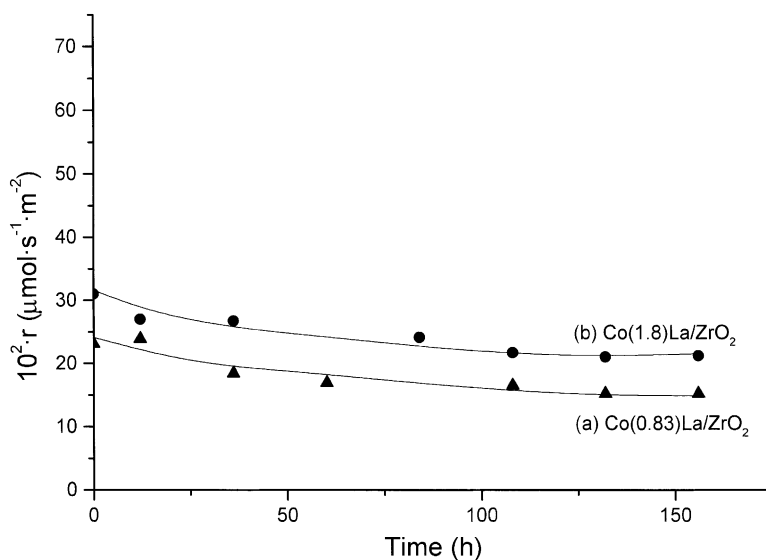

Fig. 4. Similar stability curves for Co supported on La-doped zirconia. (a) Three ALE cycles, (b) five ALE cycles.
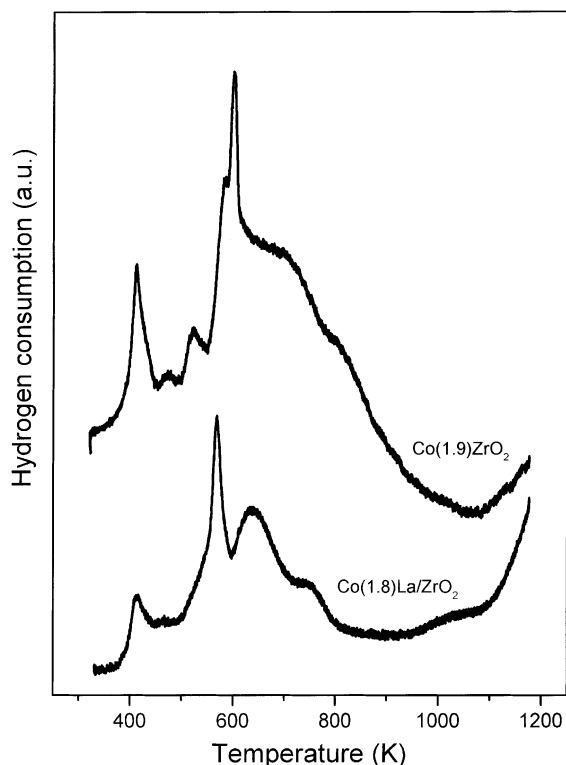
Fig. 5. TPR profiles of Co supported on La/ZrO$_2$ and ZrO$_2$. 5% H$_2$ in Ar, 40 cm^3(STP) min^{-1} and 10 K min^{-1}.

up to 1170 K that could correspond to cobalt strongly interacting with the supports. In fact, the TPR profile of the ZrO$_2$ support is flat and does not hint the start of a reduction peak around 1170 K. The existence of hard-to-reduce species is further confirmed by the total H$_2$ consumption up to 1170 K (Table 3). Note that the lowest values pertain to La-doped systems. Also note the difference in H$_2$/Co consumption between Co(1.9)/ZrO$_2$ and Co(1.9)ZrO$_2$ indicating that the interaction between the transition metal and the support is stronger for the impregnated solid.

TPR experiments could not be done over aged catalysts due to the small amount of solid used. Instead, water annealed Co(0.42)ZrO$_2$ and Co(0.38)La/ZrO$_2$ (treated at 970 K for more than 150 h in steam saturated air) were analyzed by TPR. No differences between fresh and water-annealed samples were found.

3.4. Surface characterization

3.4.1. Fresh catalysts

The surface Co/(La + Zr) ratio increases with the number of ALE reaction cycles for cobalt supported on both ZrO$_2$ and La/ZrO$_2$ (Table 3). Nevertheless, the increase is higher from the first to the third cycle than from the latter to the fifth. Accordingly, the same

Table 3
Surface characterization

Catalysts	Wt.% Co (x)	H$_2$/Co[a] fresh	Surface atomic Co/(Zr + La) ratio		Zr 3d$_{5/2}$[b] BE (eV)		Co 2p$_{3/2}$[b] BE (eV)	
			Fresh	Aged[c]	Fresh	Aged[c]	Fresh	Aged[c]
Co(x)La/ZrO$_2$	1.8	0.8	0.15	0.13	182.9	182.8	780.8	781.0
	0.83	0.8	0.13	0.07	182.7	182.7	780.9	780.8
	0.38	0.9	0.07	–	182.7	–	781.0	–
Co(x)ZrO$_2$	1.9	1.2	0.14	–[d]	182.4	182.6	781.1	–[d]
	0.95	1.3	0.12	–	182.7	–	781.6	–
Co(x)/ZrO$_2$	1.9	1.0	0.13	–[d]	182.7	182.1	781.0	–[d]
			Fresh	H$_2$O annealed[e]	Fresh	H$_2$O annealed[e]	Fresh	H$_2$O annealed[e]
Co(x)La/ZrO$_2$	0.38	0.9[f]	0.07	–[d]	182.7	182.9	781.0	–[d]
Co(x)ZrO$_2$	0.42	1.4[f]	0.07	–[d]	182.8	182.4	781.2	–[d]

[a] TPR data: 5% H$_2$ in Ar, 40 cm^3(STP) min^{-1}, 10 K min^{-1} (320–1170 K).

[b] Binding energies corrected using the value of 530.0 eV for the O 1s peak (lattice oxygen).

[c] Aging treatment: 150 h on stream at 970 K.

[d] Very weak noisy cobalt signal that could not be quantified.

[e] Hydrothermal treatment: Catalysts were kept at 970 K for more than 150 h in flowing wet air (3% H$_2$O).

[f] No difference between fresh and water annealed samples.

tendency was observed for the initial reaction rates at 770 K (Fig. 1).

Co $2p_{3/2}$ photoelectron spectra obtained for the different supported oxides exhibit the presence of Co^{2+}, as revealed by the shake-up peaks that could be associated with the small low temperature peak observed on the TPR profiles. A more comprehensive XPS study of the Co 2p signal has been reported elsewhere [11]. It included lower cobalt contents and, for comparison, cobalt impregnated on La_2O_3, which only shows the presence of Co^{3+}. The binding energies (BE) of Co $2p_{3/2}$ seem to be slightly lower for Co in Co(x)La/ZrO$_2$ than for Co in Co(x)ZrO$_2$ samples (Table 3). This difference is in the direction expected if lanthanum is interacting with cobalt. It is well known that these two elements react to form LaCoO$_3$ perovskite and the Co $2p_{3/2}$ BE for this compound is 779.7 eV. On the other hand, no tendencies are observed for Zr $3d_{5/2}$ BE.

3.4.2. Used catalysts

3.4.2.1. Aged catalysts. The atomic surface Co/(Zr+ La) ratio for Co(1.8)La/ZrO$_2$ is slightly lower than that of the fresh catalyst (Table 3 and Fig. 6a). A larger decrease was recorded for Co(0.83)La/ZrO$_2$ (Table 3).

The XPS spectra for Co(1.9)ZrO$_2$ and Co(1.9)/ZrO$_2$ show a drastic decrease in the amount of surface cobalt (Table 3 and Fig. 6b). These results are consistent with their sharp drop in catalytic activities during the aging treatment (Fig. 2).

3.4.2.2. Water annealed catalysts. In what concerns to hydrothermally aged catalysts, cobalt was detected neither on the surface of Co(0.42)ZrO$_2$ nor on Co(0.38)La/ZrO$_2$. Probably, the detection limit of this technique did not allow us to find differences between the cobalt exposed on both solids (Table 3).
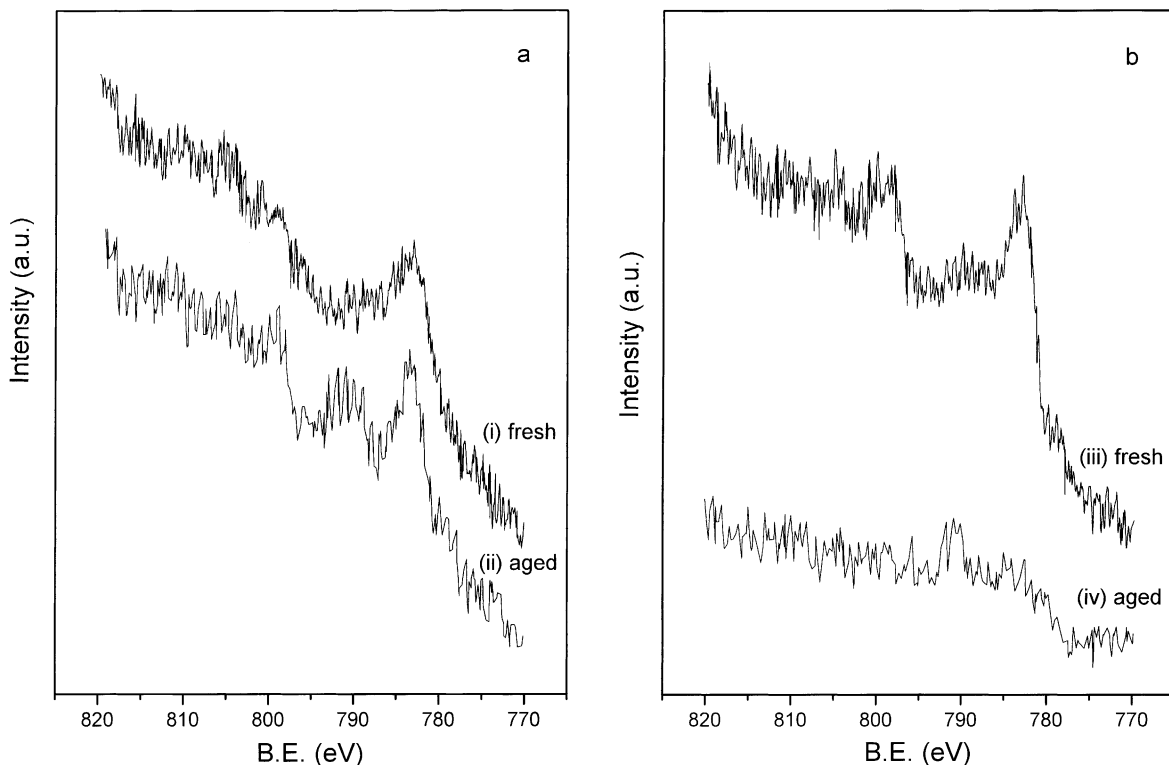

Fig. 6. XPS Co 2p core level spectra of: (a) Co(1.8) La/ZrO$_2$ (i) fresh, (ii) after stability test. (b) Co(1.9)ZrO$_2$ (iii) fresh, (iv) after stability test.

4. Discussion

4.1. Nature of surface cobalt

The catalysts were prepared by applying one to five sequential $Co(acac)_3$ chemisorptions to the surface with calcination steps between them. During the chemisorption, it is proposed that $Co(acac)_3$ is attached to the surface OH losing an acac-ligand, while the other two acac-ligands are oxidized during calcination. This means that after one ALE cycle, Co remains bonded to the support through an oxygen, producing Co monoatomic islands [15–17]. However, in the following ALE cycles, $Co(acac)_3$ could not only react with hydroxyls from the support but also with the OH groups of the Co–OH species previously generated. In this way the Co monoatomic patches are extended and Co polyatomic islands are formed [15]. The difference between these two types of Co sites is that the Co in the former case interacts with the support and in the latter case with Co.

The Kerkhof–Moulijn model [18], simplified by León [19], led us to conclude that beyond the first ALE cycle in $Co(x)ZrO_2$ mostly polyatomic islands were formed on the external surface area of ZrO_2 grains (estimated to be 40% of the total surface area) [11]. The XPS model is entirely consistent with the catalytic results, i.e. the initial reaction rates do not increase proportionally to the cobalt loadings (Fig. 1). Even though it is not possible to apply this model to the $Co(x)La/ZrO_2$ system due to the heterogeneity of the surface, the XPS results and catalytic activities conform to the same picture.

The TPR experiments in the fresh catalysts hint the presence of a high-temperature reduction peak that starts to develop at temperatures higher than 1070 K (Fig. 5). In addition, the total consumption H_2 is in all cases below 1.5 H_2/Co and in some cases as low as 0.8. These results are symptomatic of the existence of a third kind of cobalt. This cobalt is the one that migrates inside the support strongly interacting with ZrO_2. This migration would be favored during the calcination steps. A similar evolution leading to the formation of cobalt silicates was reported by Backman et al. [16,17] when Co/SiO_2 was prepared using the ALE technique and calcined at temperatures above 770 K.

It is then proposed that three kinds of cobalt species exist on zirconia supported cobalt catalysts: (i) monolayer patches, (ii) multilayer agglomerates and (iii) bulk cobalt ions strongly interacting with ZrO_2. Let us see how the catalytic and additional XPS data help refine this model.

4.2. Surface cobalt stability

Initially, the most active solid is $Co(1.9)ZrO_2$ (Fig. 1). Nevertheless, its activity sharply decreases during the stability test (Fig. 2). After 150 h on stream this solid approaches the performance of the impregnated solid ($Co(1.9)/ZrO_2$).

Both $Co(0.42)ZrO_2$ and $Co(1.9)ZrO_2$ are solids prepared by ALE in which the only difference is the number of ALE cycles, reflected in the cobalt loadings. Fig. 3 shows the evolution of these two catalysts with time on stream. $Co(1.9)ZrO_2$ decays faster than $Co(0.42)ZrO_2$. Beyond 150 h on stream they might coincide if one extrapolates both curves. So it seems that the fresh catalysts exhibit a completely different cobalt distribution but after 150 h on stream their surfaces do not seem to differ considerably. According to the previous analysis the deactivation should be a consequence of cobalt migration inside the zirconia lattice. The XPS data (Table 3 and Fig. 6b) confirm the disappearance of cobalt from the surface of the aged catalysts prepared by either the ALE or the conventional impregnation method. There is of course a low concentration of exposed cobalt sites which are "detected" by the combustion reaction but too low to be seen with our XPS instrument.

Comparing now the three solids with similar wt.% Co ($Co(1.9)ZrO_2$, $Co(1.9)/ZrO_2$ and $Co(1.8)La/ZrO_2$), note that the latter is much more stable (Fig. 2). Going back to Table 3 and Fig. 6a the XPS data still show the presence of exposed cobalt on this catalyst.

For cobalt supported on La/ZrO_2, Fig. 4 shows the same relative stability for the solids containing 0.83 and 1.8 wt.% Co. The constancy in the difference of the reaction rates during the aging treatment may indicate that there is no modification in the characteristics of the active sites for the solids with three and five ALE cycles, just a slight decrease in their concentration. Accordingly, the Co/(La + Zr) atomic surface ratio of $Co(1.8)La/ZrO_2$ changes slightly after 150 h on stream

at 970 K. A decrease in surface cobalt concentration is observed for aged Co(0.83)La/ZrO$_2$ (Table 3). Its Co/(La + Zr) atomic surface ratio becomes the same as that obtained for fresh Co(0.38)La/ZrO$_2$. As expected from the model their activities are almost the same (Figs. 1 and 4).

The deactivation of the lanthanum containing catalysts is much less pronounced than those prepared with undoped zirconia. In the former case the migration of cobalt inside the bulk is retarded and a significant fraction of cobalt remains exposed on the catalyst surface. The lanthanum oxide on the catalyst surface seems to act as a stabilizer of the transition metal.

Also, the ALE technique seems to play a role in the production of Co ions strongly anchored to the La/ZrO$_2$ surface. This is supported by the specific rates measured with Co(3.3)/La$_2$O$_3$ (r = 5.4×10^{-2} μmol s^{-1} m^{-2}), and Co(0.27)La$_2$O$_3$ (r = 4.6×10^{-2} μmol s^{-1} m^{-2}) [11]. The former was prepared by wet impregnation using a solution of Co acetylacetonate in isobutyl alcohol while the latter was obtained using the ALE technique. Note that although the cobalt loadings differ by an order of magnitude, the reaction rates are practically the same.

4.3. Surface model

A simple model emerges for Co(x)ZrO$_2$ from the combination of instrumental and catalytic results (Fig. 7). After the first ALE cycle cobalt is anchored on the ZrO$_2$ external surface. Monoatomic islands are formed. During the next cycles progressively most of the Co is attached over cobalt (polyatomic islands grow) and Co penetration proceeds. The inside migration of Co is the cause of deactivation after the aging treatments.

In the case of Co(1.9)/ZrO$_2$, the intrinsic nature of the wet impregnation method produces from the beginning less dispersed cobalt species, and consequently, a less active solid. After the aging treatment, cobalt migrates inside ZrO$_2$ grains and the Co 2p signal becomes invisible in our XPS instrument (Fig. 6b). In fact this catalyst have lost 75% of its initial low activity.

In the fresh Co(x)La/ZrO$_2$ samples, the three kinds of Co species are present. Although, the catalytic activity for the one ALE cycle sample, Co(0.38)La/ZrO$_2$, is close to that of Co(0.42)ZrO$_2$ (both have monoatomic islands), the reaction rates for the three and five ALE

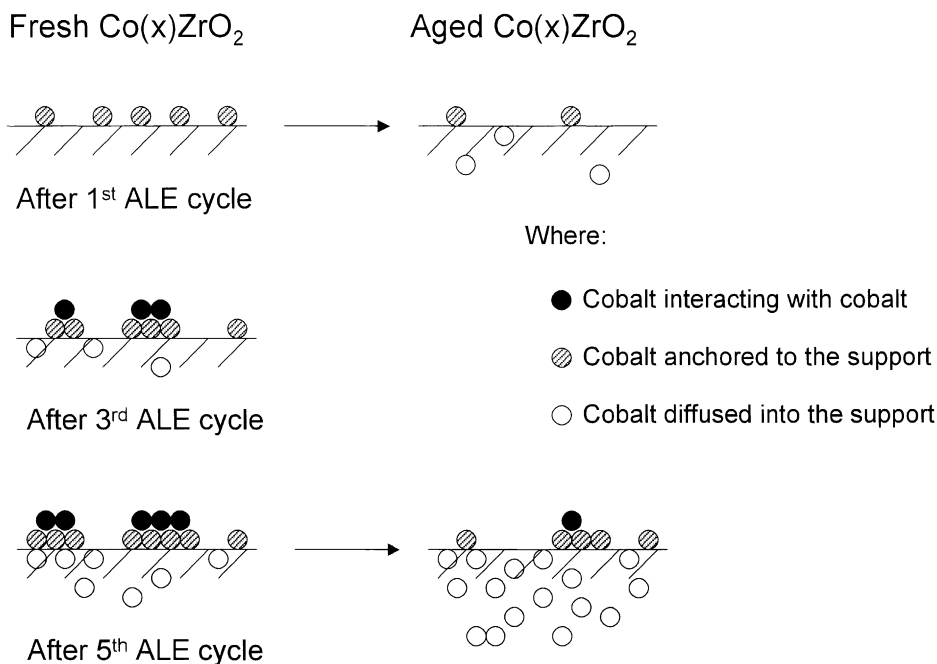Fig. 7. Schematic model for fresh and aged catalysts.

cycle samples are lower than those of Co(x)ZrO$_2$ with the same ALE cycles, suggesting that lanthanum would interact with Co in the polyatomic islands. It is known that cobalt oxides and La$_2$O$_3$ strongly interact to form stable mixed oxides. We could not detect their formation at the bulk level (XRD) although both TPR and XPS data might hint such an interaction. The beneficial effect of La doping is reflected by the retention of exposed cobalt (Table 3 and Fig. 6a) that in turn avoids sharp deactivation of these catalysts after 150 h on stream at 970 K.

5. Conclusions

The anchoring effect of lanthanum leads to the production of a stable Co(x)La/ZrO$_2$ catalyst for methane combustion at high temperatures (150 h on stream at 970 K). This effect is enhanced by the use of a preparation technique (ALE) that leads to a better surface distribution of cobalt.

Both the instability of non-doped Co(x)ZrO$_2$ (ALE method) and Co(x)/ZrO$_2$ (impregnation method) and the increased deactivation resistance of lanthanum containing formulation has been rationalized in terms of a simple model mainly supported by the surface properties revealed by XPS.

Acknowledgements

References

[1] D.L. Trimm, Appl. Catal. 7 (1983) 249.
[2] H. Arai, H. Fukuzawa, Catal. Today 26 (1995) 217.
[3] R.M. Heck, R.J. Farrauto, Catalytic Air Pollution Control, Commercial Technology, Van Nostrand, Princeton, NJ, 1995.
[4] H. Arai, K. Eguchi, M. Machida, T. Shiomitsu, Catal. Sci. Tech. 1 (1991) 195.
[5] J.C. van Giezen, M. Intven, M.D. Meijer, J.W. Geus, A. Mulder, G.J. Riphagen, J.P. Brouwer, Catal. Today 47 (1999) 191.
[6] Z.R. Ismagilov, R.A. Shkrabina, N.A. Koryabkina, Catal. Today 47 (1999) 51.
[7] J.G. McCarty, M. Gusman, D.M. Lowe, D.L. Hildenbrand, K.N. Lau, Catal. Today 47 (1999) 5.
[8] P. Euzen, J. Le Gal, B. Rebours, G. Martin, Catal. Today 47 (1999) 19.
[9] R.A. Dalla Betta, Catal. Today 35 (1997) 129.
[10] V.G. Milt, M.A. Ulla, E.A. Lombardo, Catal. Lett. 65 (2000) 67.
[11] V.G. Milt, M.A. Ulla, E.A. Lombardo, J. Catal. 200 (2001) 241.
[12] D. Klavana, J. Kirchnerová, J. Chaouki, J. Delval, W. Yaïci, Catal. Today 47 (1999) 115.
[13] C. Batiot-Dupeyrat, F. Martinez-Ortega, M. Ganne, J.M. Tatibouët, App. Catal. A: Gen. 206 (2001) 205.
[14] J.J. Carberry, Chemical and Catalytic Reaction Engineering, McGraw-Hill, New York, 1976, pp. 205–233.
[15] A. Kytökivi, J. Jacobs, A. Hakuli, J. Merilainen, H. Brongersma, J. Catal. 162 (1996) 190.
[16] L.B. Backman, A. Rautiainen, M. Lindblad, A.O.I. Krause, Appl. Catal. A: Gen. 191 (2000) 55.
[17] L.B. Backman, A. Rautiainen, M. Lindblad, O. Jylhä, A.O.I. Krause, Appl. Catal. A: Gen. 208 (2001) 223.
[18] F.P.J.M. Kerkhof, J.A. Moulijn, J. Phys. Chem. 83 (1979) 1612.
[19] V. León, Surf. Sci. 339 (1995) L931.